Published in final edited form as:
J Nanopart Res. 2011 October ; 13(10): 5547–5555. doi:10.1007/s11051-011-0544-3.

Cerium oxide and platinum nanoparticles protect cells from oxidant-mediated apoptosis

Andrea Clark[1], **Aiping Zhu**[1], **Kai Sun**[2], and **Howard R. Petty**[1,*]

[1]Department of Ophthalmology and Visual Sciences, The University of Michigan Medical School, Ann Arbor, MI 48105

[2]Department of Materials Science and Engineering, The University of Michigan, Ann Arbor, MI 48109

Abstract

Catalytic nanoparticles represent a potential clinical approach to replace or correct aberrant enzymatic activities in patients. Several diseases, including many blinding eye diseases, are promoted by excessive oxidant stress due to reactive oxygen species (ROS). Cerium oxide and platinum nanoparticles represent two potentially therapeutic nanoparticles that de-toxify ROS. In the present study we directly compare these two classes of catalytic nanoparticles. Cerium oxide and platinum nanoparticles were found to be 16±2.4 nm and 1.9±0.2 nm in diameter, respectively. Using surface plasmon enhanced microscopy, we find that these nanoparticles associate with cells. Furthermore, cerium oxide and platinum nanoparticles demonstrated superoxide dismutase catalytic activity, but did not promote hemolytic or cytolytic pathways in living cells. Importantly, both cerium oxide and platinum nanoparticles reduce oxidant-mediated apoptosis in target cells as judged by the activation of caspase 3. The ability to diminish apoptosis may contribute to maintaining healthy tissues.

Keywords

Catalytic nanoparticles; reactive oxygen metabolites; cell toxicity; apoptosis

Introduction

Biomimetic characteristics have been described for several nanoparticles. For example, nanocomposites made of gold and platinum exhibit bacterial-like motility by asymmetrically catalyzing the conversion of hydrogen peroxide to oxygen (Paxton et al., 2004). Nanoparticles may also display enzymologic properties, such as peroxidase, oxidase, catalase, and superoxide dismutase activity (e.g., Gao et al., 2007; Korsvik et al., 2007). Superoxide dismutase activity has been ascribed to nanoceria. Indeed, the “superoxide dismutase” catalytic rate constant of nanoceria exceeds that the of the native biological enzyme superoxide dismutase (Korsvik et al., 2007). Nanoceria are catalysts with mixed valency properties; cerium is found in both +3 and +4 oxidation states (Bumajdad et al., 2009; Deshpande et al., 2005; Mamontov and Egami, 2000). Nanoceria act catalytically by regenerating oxidation states (Chen et al., 2006; Das et al., 2007; Tarnuzzer et al., 2005; Schubert et al., 2006; Niu et al., 2007; Korsvik et al., 2007). The protective effects of nanoceria are well documented (Chen et al., 2006; Chen et al., 2006; Das et al., 2007;

*Address editorial correspondence and reprint requests to: Dr. Howard R. Petty, Department of Ophthalmology and Visual Sciences, 1000 Wall Street, The University of Michigan Medical School, Ann Arbor, MI 48105, Phone: 734-647-0384/fax:734-936-3815/ hpetty@umich.edu.

Tarnuzzer et al., 2005; Schubert et al., 2006; Niu et al., 2007; Korsvik et al., 2007; Colon et al., 2009; Elswaifi et al., 2009; Singh et al., 2007). Recently, nanoceria have been shown to prevent vision loss in an animal model of light-induced photoreceptor degeneration (Chen et al., 2006). Similarly, platinum nanoparticles have been shown to scavenge ROS (Hamasaki et al., 2008; Kajita et al., 2007; Watanabe et al., 2009; Hikosaka et al., 2008). In vitro cell studies have shown that platinum nanoparticles deflect cell damage and reduce cell death due to oxidant exposure (Kim et al., 2009; Zhang et al., 2010). Furthermore, the anti-oxidant capacity of platinum nanoparticles has been used to influence pulmonary inflammation in mice and extend the lifetime of *C. elegans* (Onizawa et al., 2009; Kim et al., 2008, 2010).

Catalytic nanoparticles offer the potential to perform enzymatic replacement therapy without the need for unproven gene replacement technology. For example, a reduction in anti-oxidant defense mechanisms is a key contributory factor in the progression of blindness in diabetic retinopathy. Genetic enhancement of superoxide dismutase expression in a rat model of diabetes mitigates oxidative damage of the retina and consequent retinopathy (Kowluru et al., 1997, 2001, 2003, 2006; Caldwell et al., 2005; Kanwar et al., 2007). Thus, it seems likely that nanotherapies aimed at replacing or augmenting anti-oxidative activity in tissues could save eyesight in millions of people.

Although cerium oxide and platinum nanoparticles have been previously studied in vitro, it is surprising that their biological properties have never been directly compared. With a view toward developing experimental nanotherapeutics, we have performed parallel experiments using cerium oxide and platinum nanoparticles. Both cerium oxide and platinum nanoparticles diminish hydrogen peroxide-mediated apoptosis without promoting cell lysis.

Materials and Methods

Materials

Cerium oxide nanoparticles were obtained from Nanoscale Corp. (Manhattan, KS). Cell culture media, Hank's balanced salt solution (HBSS), and Calcein-AM were purchased from Invitrogen (Carlsbad, CA). The CaspGLOW red active caspase-3 staining kit was obtained from BioVision (Mountain View, CA). Cover-glass bottom dishes were purchased from MatTek Corporation (Ashland, MA). Unless otherwise noted, chemicals were obtained from Sigma Chemical Company (St. Louis, MO).

Preparation of platinum nanoparticles

Platinum nanoparticles were prepared by an established protocol utilizing the alcohol reduction of $PtCl_6^{-2}$ (Watanabe et al., 2009; Shiraixhi et al., 2000) with some modifications. Briefly, 0.62g of polyacrylic acid partial sodium salt (M_w = 2000, 61–65 wt. % in H_2O) was diluted to 25 ml with water, and 13.6 mg of $PtCl_6^{-2}$ was added. Twenty-five ml of ethanol was then added to the mixture during magnetic stirring. The yellow solution was heated to reflux for 4 hr and then cooled to room temperature. The solvents were removed and the resultant black solid was dispersed in water.

Nanoparticle suspensions

Nanoparticles were suspended in HBSS, and maintained at 4 °C. Working dilutions of 1.2 mg/ml and 1.7μg/ml were made for platinum and cerium nanoparticles, respectively. All suspensions were vortexed before use.

HT-1080 cell culture

The HT-1080 human breast fibrosarcoma cell line (American Type Cell Culture Collection CCL-121, Marassas, VA) was maintained on plastic tissue culture flasks in Dulbecco's

modified Eagle medium (DMEM, Invitrogen) containing 10% heat-inactivated FBS (Invitrogen) and 1% antibiotic/antimycotic (Invitrogen). Cells were detached using a trypsin/EDTA solution (Invitrogen), transferred to fresh media, and plated onto glass cover slips 24 hr prior to use. For cytolysis and apoptosis assays, cells were plated into 96 well cell culture plates (Costar 3595, Corning Inc., Corning, NY).

Hemolysis assay

Peripheral blood was collected from healthy human donors in compliance with the guidelines of the University of Michigan Institutional Review Board for Human Subject Research. Red blood cells were isolated using Ficoll-Histopaque (Sigma) density gradient centrifugation, then re-suspended and washed in HBSS by centrifugation. Cells were treated with nanoparticles for 3 hr at 37° C. Cells were centrifuged, and supernatants removed to a 96 well plate. Absorbance at 540 nm was read on a FlexStation plate reader (Molecular Devices, Sunnyvale, CA). A sample treated with 1% Triton-X 100 (Sigma) in HBSS was used as a 100% hemolysis standard.

Cytolysis assay

HT-1080 cells were seeded into 96 well cell culture plates at 10^4 cells per well and cultured overnight in DMEM. Cells were labeled with Calcein-AM (Invitrogen) for 30 min at 37° C, and washed thoroughly with HBSS. Triplicate wells were treated with cerium oxide or platinum nanoparticles at the concentrations indicated below or with 1% Triton-X 100 in HBSS to serve as a reference sample for 100% release. The plate was then incubated for 3 hr at 37° C. After incubation, supernatants were centrifuged to remove particulates. Supernatants were transferred to a fresh 96 well plate then read on a FlexStation II (Molecular Devices) using an excitation of 494 nm and emission of 517 nm. Fluorescence intensities were averaged over triplicate wells.

Oxidase activity

The oxidase-like activity of nanoparticles was assessed as described by Asati et al. (2009). Briefly, citrate buffer (80 μl, 0.1M, pH 4.0) was pipetted into individual wells of a 96-well plate (Costar 3626, Corning) followed by the addition of 10 μl of nanoparticle nanoparticles and 10 μl of freshly dispersion (1.2 mg/ml of Pt and 0.17 mg/ml of CeO_2 prepared 3,3′,5,5′-tetramethylbenzidine (TMB) (5 mM in citrate buffer) solution. These mixtures were incubated for 15 min at room temperature in the dark. Absorbance at 650 nm was measured with a plate reader (Molecular Devices). Absorbance values were corrected by subtracting the background value in the absence of nanoparticle addition from all sample readings.

Superoxide dismutase activity

The SOD assay was performed using the protocol of Ukeda et al. (1999), with some modifications. Briefly, 60 μl of carbonate buffer (0.1M, pH 9.2) and 3 mM of an EDTA solution were transferred into wells of a 96-well plate (Costar 3626, Corning) followed by the addition of 10 μl of nanoparticle dispersion or buffer solution, 10 μl of 3 mM xanthine, 10 μl of 1.0 mM WST-1 solution and 10 μl of xanthine oxidase. These mixtures were incubated for 30 min at room temperature in the dark. Absorbance at 440 nm was measured with a plate reader (Molecular Devices). Background absorbance was corrected by subtracting the value of the xanthine oxidase omission control from all sample readings.

Apoptosis assay

HT-1080 cells were seeded into cover-glass bottom dishes and allowed to grow for 24–48 hr. Cerium oxide or platinum nanoparticles were added at the concentrations indicated below and then allowed to incubate at 37° C. After 24 hr, plates were washed with HBSS,

then incubated for 3 hr at 37° C with either HBSS, or HBSS containing 200 μM H_2O_2. Plates were then stained for caspase-3, using the CaspGLOW™ red active caspase-3 staining kit (BioVision) as directed by the manufacturer. Plates were then washed and imaged using a 40x objective and an Andor iXon camera (Andor Techol., Belfast, Northern Ireland) attached to the bottom port of a Nikon TE2000-U inverted microscope with a 100W mercury lamp. Caspase-3 red labeling was observed using a Nikon 96321 filter set comprised of a 570 nm dichroic mirror, a 530–560 nm excitation filter, and a 590–650 nm emission filter.

Bright field and surface plasmon enhanced dark-field microscopy

HT-1080 cells were seeded onto cover slips and allowed to grow for 24 hr. Cover slips were treated with 17 ng/ml cerium oxide or 1.2 mg/μl platinum nanoparticles for an additional 24 hr. Cells were washed with HBSS, and then mounted live for microscopy. To permit transmitted light imaging using both bright field and surface plasmon enhanced dark field condensers in the same experiments, a two arm swing-out assembly was constructed. A CytoViva, Inc. (Auburn, AL) darkfield condenser and illumination source was attached to a standard Zeiss carrier for transmitted light illumination. To the side of the microscope, a smaller Zeiss 20 W bright field illumination system attached to an illuminator carrier (cat. no. 45 17 51) was secured by a counter-balanced and hinged stand bolted to the tabletop. A Zeiss Axiovert microscope equipped with a 100× darkfield objective (Olympus) and an epifluorescence condenser was employed. Surface plasmon enhanced microscopy produces a very high contrast image of very high optical resolution (90 nm) (Vainrub et al., 2006). To preserve resolution, a 1.9× Optem camera coupler (Qioptiq Imaging Solutions, Fairport, NY) was used to direct the image to a large format (4096 × 4096) Alta-U16M camera (Apogee Imaging Systems, Roseville, CA). The camera was liquid-cooled to reduce the dark noise and to minimize physical vibrations due to cooling. This arrangement preserves high sample resolution by providing an optimal pixel size according to the Nyquist sampling criterion while also providing a high 91K well capacity. Images were downloaded for further processing using Metamorph software (Molecular Devices).

Electron microscopy

Transmission electron microscopy images were obtained with a 200 kV JEOL 2010F microscope, as previously described (Chen et al., 2011).

Results

Nanoparticles

Cerium oxide (Chen et al., 2006; Das et al., 2007; Tarnuzzer et al., 2005; Schubert et al., 2006; Niu et al., 2007; Korsvik et al., 2007) and platinum (Watanabe et al., 2009; Shiraixhi et al., 2000) nanoparticles have been thoroughly described in the literature. To confirm certain characteristics of these nanoparticles, transmission electron microscopy studies were performed. Fig. 1A shows TEM images of cerium oxide nanoparticles purchased from a commercial source. They were found to have a diameter of 16±2.4 nm. Fig. 1B shows TEM images of platinum nanoparticles prepared as described by Watanabe et al. (2009). These platinum nanoparticles were found to have a 1.9±0.2 nm diameter. In addition, it was noted that the agglomeration state of cerium oxide nanoparticles was greater than that of platinum nanoparticles. These properties are consistent with those previously reported.

Observation of Catalytic Nanoparticles in Vitro

After a 24 hr growth period on cover slips, cells were treated with 17 ng/ml cerium oxide or 1.2 μg/ml platinum nanoparticles for an additional day. Cells were then washed with HBSS.

To determine if cerium oxide and platinum nanoparticles associate with cells or are in their vicinity, microscopy experiments were performed. One means of detecting nanoparticles in vitro, particularly those with electronic conduction bands, is surface plasmon enhanced darkfield microscopy. Fig. 2 shows conventional brightfield and surface plasmon enhanced darkfield microscopy of cells. Column 1 shows images of an untreated cell. No intensely scattering particles are apparent. In contrast, cells treated with cerium oxide (column 2) or platinum nanoparticles (column 3) display intense and punctate light scattering due to nanoparticles (arrows). The nanoparticles did not appear to label a specific cell compartment. Hence, cerium oxide and platinum nanoparticles associate with living cells.

Enzymatic Activities

To confirm that the nanoparticles used in subsequent experiments express enzymatic activity, we first assessed oxidase-like activity using the method of Asati et al. (2009). For platinum nanoparticles (10 μl, 1.2 mg/ml), a value of $\Delta A=0.1339\pm0.0118$ (n=3) (equivalent to 1.63±0.12 μM WST-1 formazan) was obtained. In the case of cerium oxide (10 μl, 0.17 mg/ml), a value of $\Delta A=0.0.967\pm0.0118$ (n=3) (equivalent to 0.1±0.01 μM WST-1 formazan) was found. Hence, both nanoparticles exhibit oxidase-like activity.

We next tested the SOD activity of cerium oxide and platinum nanoparticles. In the absence of SOD-like activity, superoxide generated by xanthine/xanthine oxidase reduces WST-1 to water-soluble formazans, which absorb at 440 nm (Ukeda et al., 1999). However, the presence of catalytic nanoparticles decreases this reaction by removing superoxide. Fig. 3 shows the nanoparticle concentration-dependent inhibition of formazan formation. These concentrations were chosen as significant SOD inhibitory activity was observed. Although both platinum nanoparticles (Fig. 3A) and cerium oxide nanoparticles (Fig. 3B) exhibit SOD activity, cerium oxide nanoparticles exhibit a greater level of enzymatic activity. However, this is based upon nanoparticle weight, which does not account for the use of PAA in platinum nanoparticle preparation. When compared to an SOD calibration curve (data not shown), 0.48 mg/ml platinum nanoparticles and 0.024 mg/ml cerium oxide exhibit roughly the activity level of 10 U/ml biological SOD.

Hemolysis and cytotoxicity

As nanoceria and platinum nanoparticles may have untoward effects on cells, we examined the potential toxicity of these nanoparticles. For example, the nanoparticles might cause the plasma membrane to rupture. To examine this possibility, we tested the ability of nanoparticles to induce the rupture of erythrocytes. Human erythrocytes were treated with nanoparticles at the various concentrations indicated (Fig. 4) for 3 hr at 37°C. Cells in buffer only were used as negative controls while Triton-X 100-treated erythrocytes were used as a measure of 100% hemolysis. After exposure to 0.17 ng/ml and 1.7 ng/ml cerium oxide or 12 ng/ml and 120 ng/ml platinum nanoparticles for 3 hr., no hemolysis could be detected (Fig. 4). Hence, these catalytic nanoparticles do not appear to affect the integrity of erythrocyte membranes.

Although cerium oxide and platinum nanoparticles do not cause the overt rupture of erythrocyte membranes, it is possible that they promote the rupture of nucleated cell membranes by other mechanisms. To determine if nanoparticles cause cytoplasm to leak from cells, the cytoplasm was labeled with the fluorescent marker Calcein-AM. HT1080 cells were labeled with Calcein-AM as we have previously described (Clark et al., 2006), then used in the marker-release assay. Control cells were treated with buffer alone. As a positive control for Calcein release, cells were treated with 1% Triton X100 (Fig. 5). After a 3 hr incubation with cerium oxide (0.17 ng/ml and 1.7 ng/ml) or platinum (12 ng/ml and 120 ng/ml) nanoparticles, no cytotoxicity was observed (Fig. 5). This range of concentrations

was chosen as it corresponds to biological activity (see below). Hence, these nanoparticles exhibited immeasurable levels hemolytic and cytolytic activity.

Apoptosis

We next evaluated the ability of cerium oxide and Pt nanoparticles to protect cells from H_2O_2-mediated apoptosis. In these experiments caspase-3 activation was measured using the CaspGLOW™ red active caspase-3 staining kit, a cell membrane-permeable dye consisting of a fluorogenic dye and a DEVD moiety specific for caspase-3. Samples were incubated with CaspGLOW™ red active caspase-3 substrate in the dark for 30 min, then washed with HBSS and observed using fluorescence microscopy. The fluorescence labeling of activated caspase-3 was quantified. After an overnight incubation with cerium oxide or platinum nanoparticles, cells were treated with H_2O_2 (200 μM) or buffer for 3 hr. Cells treated with only 200 μM H_2O_2 demonstrate high levels of apoptosis (~40%) compared with the low levels of apoptosis (~5%) found for cells treated with buffer alone (Fig. 6). Fig. 6 shows that cerium oxide and Pt nanoparticles protect cells from H_2O_2-induced apoptosis. Although H_2O_2 causes a dramatic increase in the percentage of caspase-3 positive cells, this can be significantly reduced by treatment with catalytic nanoparticles. Hence, both cerium oxide and Pt nanoparticles diminish H_2O_2-induced apoptosis.

Discussion

Reactive oxygen species (ROS) such as superoxide anions, hydroxyl radicals, hydrogen peroxide and hyperchlorous acid have been linked to a broad spectrum of human diseases, including cardiovascular disease, Alzheimer's disease, amyotrophic lateral sclerosis, and diabetes. Oxidant stress is also known to play a key role in ocular diseases, such as age-related macular degeneration (AMD), glaucoma, uveitis and diabetic retinopathy (Osborn, 2010; Kawaji et al., 2011; Wu et al., 1997; Kowluru et al., 2006; Caldwell et al., 2005; Kanwar et al., 2007), which together contribute to blindness in tens of millions of people worldwide. The number of patients with retinal disease is expected to increase dramatically over the next decades; for example, in the United States alone, diabetic retinopathy patients will number 16 million by 2050 (Saaddine et al., 2008). Novel approaches to mitigate oxidative tissue damage in the aging population of the Western world must be developed.

Although nanoparticles have begun making significant inroads into medicine as contrast agents in magnetic resonance imaging, drug delivery vehicles, and mediators of directed hyperthermia, catalytic nanoparticles have not yet found a clinical niche. Enzymatic replacement therapy of superoxide dismutase activity is a potential niche for catalytic nanoparticles, as a reduction in this enzyme's activity has been linked with disease. As mentioned above, both platinum nanoparticles and cerium oxide have been proposed as potential means of managing oxidant formation in vivo, although they have never been directly compared with one another. In order to develop a nanotherapeutic enzyme replacement strategy, it is necessary to evaluate all available options. In directly comparing their enzymatic activities, we found that the superoxide dismutase activity of cerium oxide nanoparticles was greater than that of platinum nanoparticles on a weight basis. Furthermore, we also directly compared the potential toxicity of two classes of nanoparticles, as significant toxicity would disqualify a nanoparticle as a potential therapeutic agent. We found that both cerium oxide and platinum nanoparticles do not promote hemolysis or cytolysis of cells. This is consistent with previous studies suggesting that they may be useful in vivo (Chen et al., 2006; Schubert et al., 2006; Kim et al., 2008, 2010).

The principle mechanism underlying retinal cell death and consequent blindness in several diseases is apoptosis, which is also known as programmed cell death. The key event leading

to cellular apoptosis is the excessive production (or reduced removal) of ROS. To model these events, we tested the ability of cerium oxide and platinum nanoparticles to reduce hydrogen peroxide-mediated apoptosis, as judged by the activation of the key apoptosis signaling molecule caspase 3. To obtain significant levels of apoptosis in a laboratory experiments, a rather large dose of hydrogen peroxide, 200 μM, is used. Both types of nanoparticles were found to reduce apoptosis. However, the significant agglomeration of cerium oxide nanoparticles may complicate the clinical use of this material. In vivo, tissues are not likely to experience the high concentrations of oxidants used in the experiments reported above. Hence, relatively low doses of nanoparticles may be sufficient to protect tissues.

Acknowledgments

This work was supported by NIH grant EY 019986 to H.R.P.

References

Asati A, Santra S, Kaittanis C, Nath S, Perez JM. Oxidase-like activity of polymer-coated cerium oxide nanoparticles. Angew Chem Int Ed Engl. 2009; 48:2308–12. [PubMed: 19130532]

Bumajdad A, Eastoe J, Mathew A. Cerium oxide nanoparticles prepared in self-assembled systems. Adv Colloid Interface Sci. 2009; 147–148:56–66.

Caldwell RB, Bartoli M, Behzadian MA, El-Remessy AE, Al-Shabrawey M, Platt DH, Liou GI, Caldwell RW. Vascular endothelial growth factor and diabetic retinopathy: role of oxidative stress. Curr Drug Targets. 2005; 6:511–24. [PubMed: 16026270]

Chen J, Patil S, Seal S, McGinnis JF. Rare earth nanoparticles prevent retinal degeneration induced by intracellular peroxides. Nat Nanotechnol. 2006; 1:142–50. [PubMed: 18654167]

Chen Q, Lu T, Xu M, Meng C, Hu Y, Sun K, Shlimak I. Fabrication of uniform Ge-nanocrystals embedded in amorphous SiO2 films using Ge-ion implantation and neutron irradiation methods. Appl Phys Lett. 2011; 98:073103-1–073103-3.

Clark AJ, Diamond M, Elfline M, Petty HR. Calicum microdomains form within neutrophils at the neutrophil-tumor cell synapse: Role in antibody-dependent target cell apoptosis. Cancer Immunol Immunother. 2010; 59:149–59. [PubMed: 19593564]

Colon J, Herrera L, Smith J, Patil S, Komanski C, Kupelian P, Seal S, Jenkins DW, Baker CH. Protection from radiation-induced pneumonitis using cerium oxide nanoparticles. Nanomedicine. 2009; 5:225–31. [PubMed: 19285453]

Das M, Patil S, Bhargava N, Kang JF, Riedel LM, Seal S, Hickman JJ. Auto-catalytic ceria nanoparticles offer neuroprotection to adult rat spinal cord neurons. Biomaterials. 2007; 28:1918–25. [PubMed: 17222903]

Deshpande S, Patil S, Kuchibhatia SVNT, Seal S. Size dependency variation in lattice parameter and valency states in nanocrystalline cerium oxide. Appl Phys Lett. 2005; 87:133113-1–133113-3.

Elswaifi SF, Palmieri JR, Hockey KS, Rzigalinski BA. Antioxidant nanoparticles for control of infectious disease. Infectious Disorders–Drug Targets. 2009; 9:445–52. [PubMed: 19689385]

Gao L, Zhuang J, Nie L, Zhang J, Zhang Y, Gu N, Wang T, Feng J, Yang D, Perrett S, Yan X. Intrinsic peroxidase-like activity of ferromagnetic nanoparticles. Nat Nanotechnol. 2007; 2:577–83. [PubMed: 18654371]

Hamasaki T, Kashiwagi T, Imada T, Nakamichi N, Aramaki S, Toh K, Morisawa S, Shimakoshi H, Hisaeda Y, Shirahata S. Kinetic analysis of superoxide anion radical-scavenging and hydroxyl radical-scavenging activities of platinum nanoparticles. Langmuir. 2008; 24:7354–64. [PubMed: 18553993]

Hikosaka K, Kim J, Kajita M, Kanayama A, Miyamoto Y. Platinum nanoparticles have an activity similar to mitochondrial NADH:ubiquinone oxidoreductase. Colloids and Surfaces B: Biointerfaces. 2008; 66:195–200.

Kajita M, Hikosaka K, Iitsuka M, Kanayama A, Toshima N, Miyamoto Y. Platinum nanopaticle is a useful scavenger of superoxide anion and hydrogen peroxide. Free Radical Res. 2007; 41:615–26. [PubMed: 17516233]

Kanwar M, Chan PS, Kern TS, Kowluru RA. Oxidative damage in the retinal mitochondria of diabetic mice: possible protection by superoxide dismutase. Invest Ophthalmol Vis Sci. 2007; 48:3805–11. [PubMed: 17652755]

Kawaji T, Elner VM, Yang DL, Clark A, Petty HR. Nuclear translocation of glyceraldehyde 3-phosphate dehydrogenase in human retinal pigment epithelium induced by oxidative stress. Redox Reports. 2011; 16:24–26.

Kim J, Takahaski M, Shimizu T, Shirasawa T, Kajita M, Kanayama A, Miyamoto Y. Effects of a potent antioxidant, platinum nanoparticle, on the lifespan of *Caenorhabditis elegans*. Mech Ageing Develop. 2008; 129:322–31.

Kim J, Shirasawa T, Miyamoto Y. The effect of TAT conjugated platinum nanoparticles on lifespan in a nematode *Caenorhabditis elegans* model. Biomaterials. 2010; 31:5849–54. [PubMed: 20434216]

Kim Y-J, Kim D, Lee Y, Choi SY, Park J, Lee SY, Park JW, Kwon HJ. Effects of nanoparticles saponin-platinum conjugates on 2, 4-dinitrofluorobenzene-induced macrophage inflammatory protein-2 gene expression via oxygen species production in RAW 264.7 cells. BMB Reports. 2009; 42:304–9. [PubMed: 19470246]

Korsvik C, Patil S, Seal S, Self WT. Superoxide dismutase mimetic properties exhibited by vacancy engineered ceria nanoparticles. Chem Commun (Camb). 2007; 14:1056–8. [PubMed: 17325804]

Kowluru RA, Kern TS, Engerman RL. Abnormalities of retinal metabolism in diabetes or experimental galactosemia. IV. Antioxidant defense system. Free Radic Biol Med. 1997; 22:587–92. [PubMed: 9013121]

Kowluru RA, Tang J, Kern TS. Abnormalities of retinal metabolism in diabetes and experimental galactosemia. VII. Effect of long-term administration of antioxidants on the development of retinopathy. Diabetes. 2001; 50:1938–42. [PubMed: 11473058]

Kowluru RA, Abbas SN. Diabetes-induced mitochondrial dysfunction in the retina. Invest Ophthalmol Vis Sci. 2003; 44:5327–34. [PubMed: 14638734]

Kowluru RA, Kowluru V, Xiong Y, Ho YS. Overexpression of mitochondrial superoxide dismutase in mice protects the retina from diabetes-induced oxidative stress. Free Radic Biol Med. 2006; 41:1191–6. [PubMed: 17015165]

Mamontov E, Egami T. Lattice defects an oxygen storage capacity of nanocrystalline ceria and ceria-zirconia. J Phys Chem B. 2000; 104:11110–6.

Niu J, Azfer A, Rogers LM, Wang X, Kolattukudy PE. Cardioprotective effects of cerium oxide nanoparticles in a transgenic murine model of cardiomyopathy. Cardiovasc Res. 2007; 73:549–59. [PubMed: 17207782]

Onizawa S, Aoshiba K, Kajita M, Miyamoto Y, Nagai A. Platinum nanoparticle antioxidants inhibit pulmonary inflammation in mice exposed to cigarette smoke. Pulmon Pharmacol Therap. 2009; 22:340–9.

Osborn, NM. Involvement of oxidative stress in the pathogenesis of glaucoma. In: Zierhut, M.; Cadenas, E.; Rao, NA., editors. Free Radicals in Ophthalmic Disorders. Informa Healthcare; NY: 2008.

Paxton WF, Kistler KC, Olmeda CC, Sen A, St Angelo SK, Cao Y, Mallouk TE, Lammert PE, Crespi VH. Catalytic nanomotors: autonomous movement of striped nanorods. J Am Chem Soc. 2004; 126:13424–31. [PubMed: 15479099]

Saaddine JB, Honeycutt AA, Narayan KM, Zhang X, Klein R, Boyle JP. Projection of diabetic retinopathy and other major eye diseases among people with diabetes mellitus: United States, 2005–2050. Arch Ophthalmol. 2008; 126:1740–7. [PubMed: 19064858]

Schubert D, Dargusch R, Raitano J, Chan S-W. Cerium and yttrium oxide nanoparticles are neuroprotective. Biochem Biophys Res Comm. 2006; 342:86–91. [PubMed: 16480682]

Shiraishi Y, Nakayama M, et al. Effect of quantity of polymer on catalysis and superstructure size of polymer-protected Pt nanoclusters. Inorgan Chimica Acta. 2000; 300:964–969.

Singh N, Cohen CA, Rzigalinski BA. Treatment of neurodegenerative disorders with radical nanomedicine. Ann NY Acad Sci. 2007; 1122:219–30. [PubMed: 18077575]

Tarnuzzer RW, Colon J, Patil S, Seal S. Vacancy engineered ceria nanostructures for protection from radiation-induced cellular damage. Nano Lett. 2005; 5:2573–7. [PubMed: 16351218]

Ukeda H, Kawana D, Maeda S, Sawamura M. Spectrophotometric assay for superoxide dismutase based on the reduction of highly water-soluble tetrazolium salts by xanthine-xanthine oxidase. Biosci Biotechnol Biochem. 1999; 63:485–8.

Vainrub A, Pustovyy O, Vodyanoy V. Resolution of 90 nm (λ/5) in an optical transmission microscope with an annular condenser. Optics Lett. 2006; 31:2855–2857.

Watanabe A, Kajita M, Kim J, Kanayama A, Takahashi K, Mashino T, Miyamoto Y. In vitro free radical scavenging activity of platinum nanoparticles. Nanotechnology. 2009; 20:455105–14. [PubMed: 19834242]

Wu GS, Zhang J, Rao NA. Peroxynitrite and oxidative damage in experimental autoimmune uveitis. Invest Ophthal Vis Sci. 1997; 38:1333–9. [PubMed: 9191596]

Zhang L, Luag L, Munchgesang W, Pippel E, Gösele U, Brandsch M, Knez M. Reducing stress on cells with apoferritin-encapsulated platinum nanoparticles. Nano Lett. 2010; 10:219–23. [PubMed: 20017497]

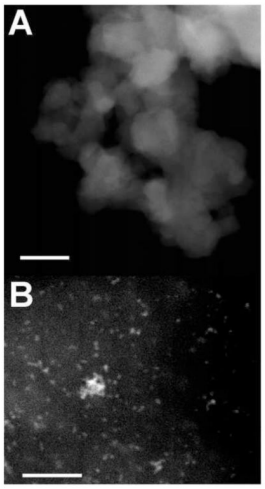

Fig. 1.
TEM images of cerium oxide and platinum nanoparticles. (A) Cerium oxide nanoparticles were 16±2.4 nm in diameter. (B) Platinum nanoparticles were 1.9±0.2 nm in diameter. (Bar=50nm)

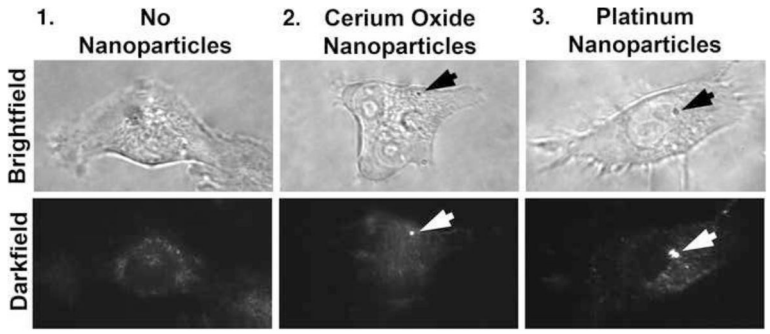

Fig. 2.

Observations of cerium oxide and platinum nanoparticles during interactions with living cells. Nanoparticles were localized using surface plasmon enhanced darkfield microscopy. The nanoparticles are observed as bright dots in the center and right-hand side panels. The resolution of the bright-field images is 240 nm whereas that of the surface plasmon-enhanced darkfield micrographs is 90 nm (Vainrub et al., 2006). (100x objective) (arrows = nanoparticles) (n=5)

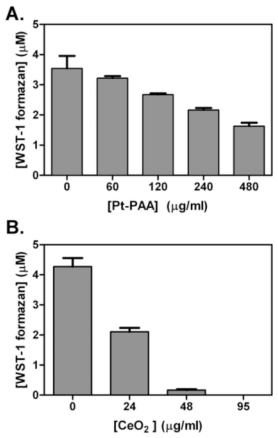

Fig. 3.

Superoxide dismutase activity is expressed by nanoparticles. The ordinate plots the amount of WST-1 formazan observed whereas the abscissa gives the nanoparticle concentration. SOD activity is illustrated by the quenching of WST-1 formazan production. This activity was measured for various concentrations of platinum nanoparticles (A) and cerium oxide nanoparticles (B). (n=3)

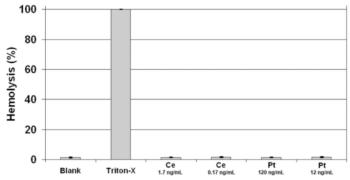

Fig. 4.

Catalytic nanoparticles do not promote hemolysis. Hemolysis was quantified spectrophotmetically by measuring the absorption of hemoglobin at 540 nm. Cerium oxide and platinum nanoparticles were incubated with erythrocytes at the concentrations indicated for 3 hr. at 37°C. No significant hemolysis could be observed. (The error bars are smaller than the size of the lines.) (n=3)

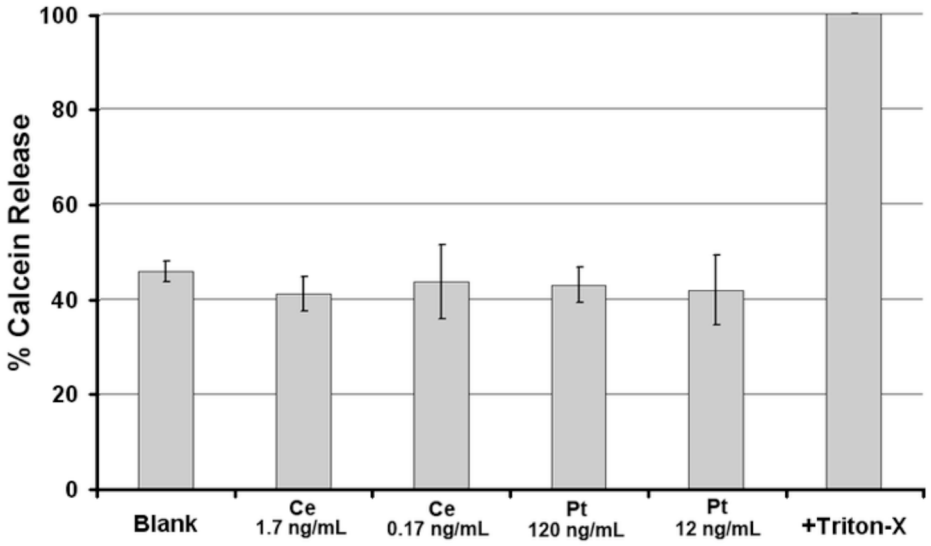

Fig. 5.

Catalytic nanoparticles do not promote cytolysis. Cytolysis was quantified using fluorescence by measuring the release of calcein into the supernatant (Invitrogen) using excitation at 494 nm and emission at 517 nm. Cerium oxide and platinum nanoparticles were incubated with cells at the concentrations indicated for 3 hr at 37°C. No significant cytolysis could be observed. (n=3)

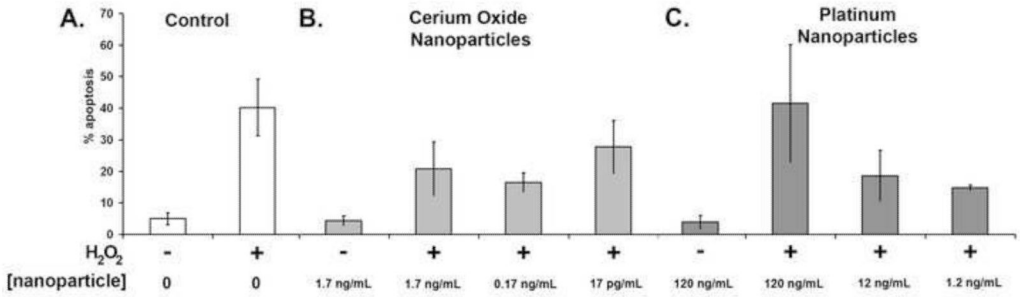

Fig. 6.

Nanoparticles protect cells from apoptosis. Cells were treated with 200 μM H_2O_2 for 3 hr at 37°C to induce apoptosis. A) Negative and positive controls are shown (left). Cerium oxide (center) and platinum (right) nanoparticles are shown in panels B and C, respectively. Significant reductions in apoptosis are seen. (*P<0.01) (n=3)